

# Prospect for measurement of CP-violation phase $\phi_s$ study in the $B_s \rightarrow J/\psi\phi$ channel at future $Z$ factory

Xiaomei Li<sup>1</sup>, Manqi Ruan<sup>2</sup>, Mingrui Zhao<sup>1\*</sup>

1.Science and Technology on Nuclear Data Laboratory, China Institute of Atomic Energy, Beijing, China/

2.Institute of High Energy Physics, Chinese Academy of Sciences, Beijing, China

## Abstracts

The CP violating phase  $\phi_s$ , the  $B_s$  decay width and the decay width difference are sensitive probe to new physics and can constrain the heavy quark expansion theory. The potential for the measurement at future  $Z$  factories is studied. It is found that operating at Tera- $Z$  mode, the expected precision can reach:  $\sigma(\phi_s) = 4.3$  mrad,  $\sigma(\Delta\Gamma) = 0.24$  ns<sup>-1</sup> and  $\sigma(\Gamma) = 0.072$  ns<sup>-1</sup>. The precision of  $\phi_s$  is competitive while a little worse than the expected resolution that could be achieved by LHCb at High-Luminosity LHC. If operating at 10-Tera- $Z$  mode, all the parameters are expected to have a better precision than what it can be measured by LHCb at High-Luminosity LHC.

## 1 Introduction

It is suggested that the New Physics may have a major impact on the CP-violating observables. The CP violation provides a powerful tool to test the Standard Model (SM). The CKM matrix describes the mixture of mass and interaction eigenstates of quarks [1, 2]. In the study of  $B_s$  meson decays, the CP-violating phase  $\phi_s$  arises from the interference between the amplitude of the  $B_s$  and  $\bar{B}_s$  decays, where the  $\bar{B}_s$  comes from the  $B_s$ - $\bar{B}_s$  oscillation. In the SM, the  $\phi_s$  can be derived as  $\phi_s = -2\beta_s$ , where the  $\beta_s \equiv \arg[-(V_{ts}V_{tb}^*)/(V_{cs}V_{cb}^*)]$ , expressed as CKM matrix elements, if the subordinate contribution is ignored.

The light (L) and heavy (H) mass eigenstates of the  $B_s$  meson have different decay widths  $\Gamma_L$  and  $\Gamma_H$ . The difference of the decay width  $\Delta\Gamma_s \equiv \Gamma_L - \Gamma_H$  and the average decay width  $\Gamma_s \equiv (\Gamma_L + \Gamma_H)/2$  are also of great interest in theory. They can be calculated using heavy quark expansion (HQE) theory [3]. The precise measurements provide a test of the HQE theory.

---

\*mingrui.zhao@mail.labz0.org

With the discovery of the Higgs boson in 2012, the Circular Electron-Positron Collider (CEPC) and Future Circular Collider (FCC-ee) projects were proposed. In addition to being designed as Higgs factories, they can also be operated in the  $Z$  pole configuration. At the  $Z$  pole, they are expected to produce  $10^{12}$  to  $10^{13}$   $Z$  bosons in 10 years. It is estimated that  $0.152 \times (10^{12} - 10^{13})$   $b\bar{b}$  pairs will be produced from  $Z$  decays. This implies that the future  $Z$ -factories are also future  $b$ -factories. The detectors (with time projection or wired chamber as the main tracker) on the CEPC and FCC-ee provide good particle identification, very precise track and vertex reconstruction, and good acceptance, making the future  $Z$ -factory a perfect place to study the heavy flavor physics.

### 1.1 Measurement of $\phi_s$ ( $\Delta\Gamma$ , $\Gamma_s$ ) in experiments

The CP -violating phase  $\phi_s$  was measured in the experiments ATLAS [4, 5], CDF [6], CMS [7], D0 [8], and LHCb [9, 10, 11, 12, 13]. In these experiments, the parameter  $\phi_s$  is extracted from a fit to the time-dependent angular distribution of  $B_s$  decays.

If the  $B_s \rightarrow J/\psi\phi$  decay channel is used, the distribution is a sum of ten terms corresponding to the four polarization amplitudes and their interference terms:

$$\frac{d^4\Gamma(B_s \rightarrow J/\psi\phi)}{dt d\Omega} \propto \sum_{k=1}^{10} h_k(t) f_k(\Omega), \quad (1)$$

where

$$h_k(t|B_s) = N_k e^{-\Gamma_s t} \left[ a_k \cosh\left(\frac{1}{2}\Delta\Gamma_s t\right) + b_k \sinh\left(\frac{1}{2}\Delta\Gamma_s t\right) + c_k \cos(\Delta m_s t) + d_k \sin(\Delta m_s t) \right]$$

$$h_k(t|\bar{B}_s) = N_k e^{-\Gamma_s t} \left[ a_k \cosh\left(\frac{1}{2}\Delta\Gamma_s t\right) + b_k \sinh\left(\frac{1}{2}\Delta\Gamma_s t\right) - c_k \cos(\Delta m_s t) - d_k \sin(\Delta m_s t) \right]$$

and  $f_k(\Omega)$  is the amplitude function.

In the expression of  $h_k(t)$ ,  $\Delta m_s$  stands for the mass difference between the  $B_s$  mass eigenstates and  $N_k$  for the amplitude of the component at  $t = 0$ . The  $\phi_s$  appear in the function as parameters, hidden in the  $a_k, b_k, c_k, d_k$  parameters. The extended expression of the parameters can be found in the LHCb publication [10]. The  $\Delta\Gamma$  and  $\Gamma_s$  can also be extracted by fitting together with  $\phi_s$ .

## 2 Estimation of resolution on the future $Z$ factory

The resolution of the measurement  $\sigma(\phi_s)$  is proportional to the inverse square root of the signal statistic. The signal statistic is proportional to the number of  $b\bar{b}$  pairs produced in a collider. And it is also proportional to the acceptance and efficiency of the detector. Two other effects have a significant impact on

resolution. One is the ability to determine the initial flavor of the  $B_s$  or  $\bar{B}_s$  meson, which is called the flavor tagging power  $p$ . The other effect is the resolution in measuring the decay time  $\sigma_t$ . It is shown that the tagging power and the resolution of the decay time affect the  $\sigma(\phi_s)$  in the formats  $\sigma(\phi_s) \propto 1/\sqrt{p}$  and  $\sigma(\phi_s) \propto 1/\exp(-\frac{1}{2}\Delta m_s^2 \sigma_t^2)$ . The effect of tagging power and time resolution on  $\sigma(\phi_s)$  is investigated in [] and validated with some toy Monte Carlo simulations. A scaling factor can be defined as

$$\xi = 1 / \left( \sqrt{N_{b\bar{b}}} \times \varepsilon \times \sqrt{p} \times \exp(-\frac{1}{2}\Delta m_s^2 \sigma_t^2) \right) \quad (2)$$

The expected  $\phi_s$  resolution measured in future  $Z$ -factories can be estimated as  $\sigma(\phi_s, \text{FE}) = \xi_{\text{FE}} \times \frac{\sigma(\phi_s, \text{EE})}{\xi_{\text{EE}}}$ . (FE: future experiment, EE: existing experiment).

The resolution and scaling factor of the existing experiment are from the LHCb studies [10]. For the LHCb measurement, the number of extracted signals is  $N_{b\bar{b}} \times \varepsilon = 117000$ . The flavor tagging power  $p$  is 4.73%. And the decay time resolution  $\sigma_t$  is at 45.5 fs. The resolution  $\sigma(\phi_s)$  is 0.041 rad. Then the scale factor  $\xi_{\text{LHCb}} = 0.018$  and the ratio  $\sigma(\phi_s)/\xi_{\text{LHCb}} = 2.28$  rad.

The scaling factor of the future  $Z$ -factory is estimated using the Monte Carlo study, which is described in detail in the following sections.

It is also worthwhile to estimate the scaling factor of the experiments at the High-Luminosity LHC. Assuming no significant changes in detector acceptance and efficiency, tagging power, and decay time resolution at HL-LHC, the scaling factor is calculated by scaling the luminosity. At HL-LHC, the expected luminosity is  $300 \text{ fb}^{-1}$ , with respect to  $1.9 \text{ fb}^{-1}$  at the current measurement of LHCb. The scaling factor is then  $\xi_{\text{HL-LHC-LHCb}} = 0.0014$  and the expected resolution is  $\sigma(\phi_s, \text{HL-LHC-LHCb}) = \xi_{\text{HL-LHC-LHCb}} \times \sigma(\phi_s)/\xi_{\text{LHCb}} = 3.2$  mrad.

The expected resolution of  $\Delta\Gamma$  and  $\Gamma_s$  is scaled in the same way from previous measurements. The key difference with  $\phi_s$  is that they are insensitive to the tagging power and proper decay time resolution. The variable

$$\zeta = 1 / \left( \sqrt{N_{b\bar{b}}} \times \varepsilon \right) \quad (3)$$

is introduced as the scaling factor for  $\Gamma_s$  and  $\Delta_s$ . The scaling factor  $\zeta_{\text{LHCb}} = 2.9 \times 10^{-3}$ ,

## 2.1 CEPC and the baseline detector

The CEPC and the baseline detector (CEPC-v4) [14] are taken as an example to study the resolution of  $\phi_s$ . As a baseline, we assume that the CEPC will run in the Tera- $Z$  mode, i.e., produces  $10^{12}$   $Z$  bosons during its lifetime. The geometry of the CEPC baseline detector consists of a vertex system, a silicon inner tracker, a TPC, a silicon external tracker, an electromagnetic calorimeter, an Hadron calorimeter, a solenoid of 3 Tesla, and a Return Yoke.

## 2.2 Monte carlo sample and reconstruction

A Monte Carlo sample is generated to study the geometry acceptance and reconstruction efficiency of the  $B_s \rightarrow J/\psi\phi$  decay channel. Another utility of this sample is to investigate the proper decay time resolution of the  $B_s$ , which is directly related to the spatial resolution of the  $B_s$  decaying vertex.

Using the WHIZARD[15] generator, about 6000  $Z \rightarrow b\bar{b} \rightarrow B_s(\bar{B}_s) + X$  events are generated. The  $B_s$  particles are then forced to decay via the  $B_s \rightarrow J/\psi(\rightarrow \mu^+\mu^-)\phi(\rightarrow K^+K^-)$  decay channel, which is performed with PYTHIA [16]. The standard configurations are used for the decay of the other particles. The transport of the particles in the detector is then simulated with MokkaC based on the GEANT4 [17] transport code. Then they are reconstructed into tracks.

The reconstructed particle species are identified with the Monte Carlo truth information. Since the detector is very good at distinguishing between leptons and hadrons, if the species of the true particle is a muon or electron, the track is identified as a lepton. And if the species of the true particle is a charged kaon, pion or proton, the track is identified as a hadron.

Further identification of the hadron as a kaon, pion, or proton is somewhat more difficult for a real detector. To avoid losing too much signal due to the efficiency of particle identification, the PID cuts are not applied in the reconstruction of the  $B_s$  particles. The  $J/\psi$  candidates are reconstructed from all combinations of a positively charged muon and a negatively charged muon, and they are selected within the window of invariant mass from 3.07 to 3.14  $\text{GeV}/c^2$ . The  $\phi$  candidates are reconstructed by all combinations of a positively charged hadron and a negatively charged hadron. The invariant mass of the  $\phi$  meson is calculated assuming that the mass of the hadron is equal to the mass of the kaon. The  $\phi$  candidate is selected within the mass window from 1.017 to 1.023  $\text{GeV}/c^2$ . The  $B_s$  meson is reconstructed over the combination of all  $J/\psi$  and  $\phi$  candidates. And these are selected within a mass window from 5.28 to 5.46  $\text{GeV}/c^2$ . After the reconstruction of the  $B_s$  meson, a decaying vertex is reconstructed with the tracks associated with the  $B_s$  particle.

The sample is also used to estimate the flavor tagging power. For this purpose, only truth-level information is passed to the flavor tagging algorithm, i.e., assuming that we have perfect particle identification.

At the same time, a sample of  $Z \rightarrow b\bar{b} \rightarrow X$  is generated to verify a low background level. The detector simulation and event reconstruction procedure are the same as for the signal.

## 2.3 Signal and background statistics

The branching fraction of  $b\bar{b}$  hadronized to  $B_s$  is 10%. At first order, we assume that all  $b\bar{b}$  events can be selected with high purity. The background in this study is the  $b\bar{b}$  events that do not contain  $B_s \rightarrow J/\psi\phi$  signal. The branching ratio of  $B_s \rightarrow J/\psi\phi$  is  $1.08 \times 10^{-3}$ . And the branching ratio of  $J/\psi \rightarrow \mu^+\mu^-$ ,  $\phi \rightarrow K^+K^-$  are 6% and 50% separately. The number of background events is

$1.7 \times 10^5$  times larger than the number of signal events. The selection criteria described in section 2.2 are applied to the background sample. It is shown that the probability of reconstructing a fake  $B_s$  candidate is  $6.7 \times 10^{-6}$ . After the event selection, background has the same magnitude as the signal, which is far from satisfactory.

The vertex information is another power variable to suppress the backgrounds. Because in the background, the candidates come from four arbitrarily combined tracks, two of which are lepton tracks and two of which are hadron tracks. Normally, the lepton has a small impact parameter and the hadron has a large impact parameter. It is difficult to reconstruct a high-quality vertex with arbitrarily combined tracks. The figure shows the  $\chi_{xy}^2$  distribution of the signal where

$$\chi_{xy}^2 = \sum_{\text{tracks}} d_{xy}^2.$$

The  $d_{xy}$  in the formula represents the distance from the reconstructed vertex to the track in the  $xy$  plane. For most signals, the vertex  $\chi_{xy}^2$  is very small. For backgrounds, on the other hand,  $\chi_{xy}^2$  is distributed over a large area. With a very loose cut at  $\chi_{xy}^2 < 0.1$ , 95% of the signals are selected and 99.2% of the backgrounds are discarded.

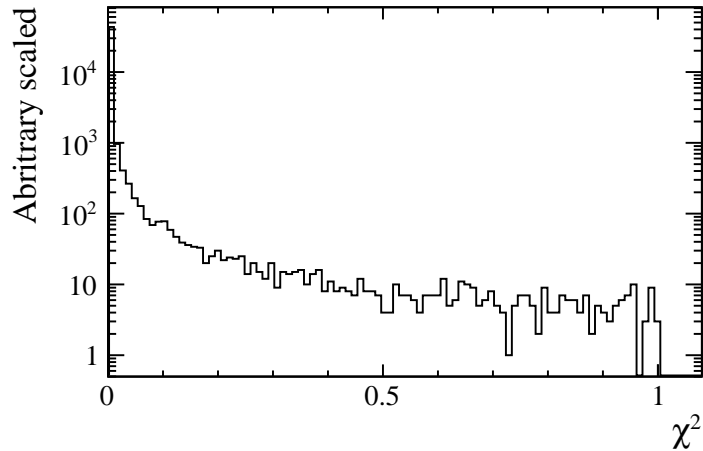


Figure 1:  $\chi_{xy}^2$  distribution of the signal.

With a combination of invariant mass and vertex cut, the acceptance and efficiency of the signal are 75%, and the background is controlled in the 1% of the signal level.

## 2.4 Flavor tagging

To extract the parameters from the equation 1, one needs to know the initial flavor ( $B_s$  or  $\bar{B}_s$ ) of the parent particle, which is called flavor tagging. In experiment, it is not always possible to determine the initial flavor, and sometimes the flavor can be determined incorrectly. The fraction of particles that could be identified (correctly or incorrectly) is called the tagging efficiency  $\varepsilon$ . The proportion of misidentified particles among the identified particles is referred to as the misidentification rate  $\omega_{\text{tag}}$ . The inability to identify the initial flavor and misidentification both reduce the ability to extract parameters from the fit. The effective statistic is lowered by a factor of  $p$  compared to perfect tagging, where

$$p = \varepsilon_{\text{tag}}(1 - 2\omega_{\text{tag}})^2.$$

### 2.4.1 Flavor tagging algorithm

A simple algorithm is developed to identify the initial flavor of the particle. Rather than knowing the limit of flavor tagging ability. The algorithm is intended to show a realistic estimate of the tagging power. The idea of the algorithm is as follows:

The  $b(\bar{b})$  quarks are predominantly produced in  $b\bar{b}$  pairs that fly to the opposite side in space. The flavor of the opposite  $b$  quark can be used to determine the initial flavor of the interested  $B_s$ . To judge the flavor of this opposite  $b$  quark, we take a lepton and a charged kaon with maximum momentum in the opposite direction of the  $B_s$ . The charge of the lepton and the kaon provides the flavor of the opposite  $b$  quark. Furthermore, when the  $b$  quark is hadronized to a  $B_s$  meson, another  $s$  quark is spontaneously created, which then has the chance to become a charged kaon, flying in the similar direction as the  $B_s$ . Based on this kaon, one can identify the flavor of the particle. The algorithm simply takes the particle with the largest momentum. If these particles provide different determinants for the flavor, the algorithm simply says that it cannot identify the flavor.

### 2.4.2 Flavor tagging power

The algorithm is applied to a Monte Carlo truth-level simulation, assuming perfect particle identification. With the tagging algorithm, the tagging efficiency is estimated as 67%. The miss-tagging rate is 22.5%. Thus, the tagging power is estimated to be 20.2%.

If the particle identification is imperfect, the flavor tagging power decreases. The effect is studied by randomly misidentifying some particles. A pion is identified as a kaon with probability  $\omega/2$ , and it has probability  $\omega/2$  to be identified as a proton. The probability of being correctly reconstructed is  $1 - \omega$ . A kaon also has a  $\omega/2$  chance of being identified as a pion and a  $\omega/2$  chance of being identified as a proton. The probability of a proton being identified as a proton or a kaon is also  $\omega/2$  in each case.

The tagging power varying with the correct particle identification rate  $1 - \omega$  is shown in Figure 2. It can be seen that the tagging power is sensitive to the  $\omega$  parameter.

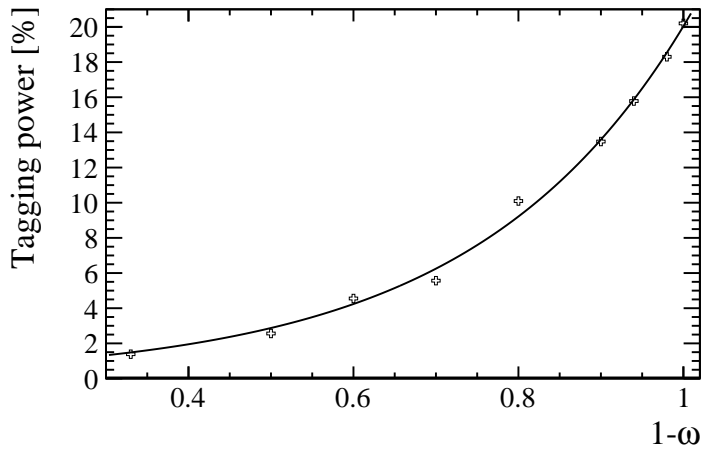


Figure 2: Tagging power as a function of the correct particle identification rate  $1 - \omega$ .

## 2.5 Time resolution

The measurement accuracy of  $\phi_s$  is affected by the inaccurate determination of the time resolution. It is powered by the factor  $\exp(-\frac{1}{2}\Delta m_s^2 \sigma_t^2)$ , where  $\sigma_t$  is the resolution of the proper decay time. The proper decay time of the  $B_s$  particle is calculated from the vertex position and momentum of the  $B_s$  particle as follows:

$$t_{xy} = \frac{ml_{xy}}{p_T},$$

where  $l_{xy} = \sqrt{x^2 + y^2}$  is the vertex position.

Figure 3 shows the distribution of the difference between  $t_{\text{reco}}$  and  $t_{\text{sim}}$ , where  $t_{\text{reco}}$  is the proper decay time calculated from the reconstructed particle information, and  $t_{\text{sim}}$  is obtained with the Monte Carlo simulated particle information without considering the detector effects.

The distribution is fitted using the sum of three Gaussian functions with the same mean value. The effective time resolution is combined as

$$\sigma_{\text{eff}} = \sqrt{-\frac{2}{\Delta m_s^2} \ln\left(\sum_i f_i e^{-\frac{1}{2}\sigma_i^2 \Delta m_s^2}\right)},$$

where  $f_i$  and  $\sigma_i$  are fraction and width of the  $i$ -th Gaussian function. The obtained effective resolution of the decay time is 4.7 fs.

The CEPC detector is expected to achieve a proper time resolution around 10 times better than the current LHCb. For one reason, the CEPC has a excellent vertex detector and a precise tracker. For another reason, the  $B_s$  produced from  $Z$ -decay is energetic resulting in a smaller proper time resolution.

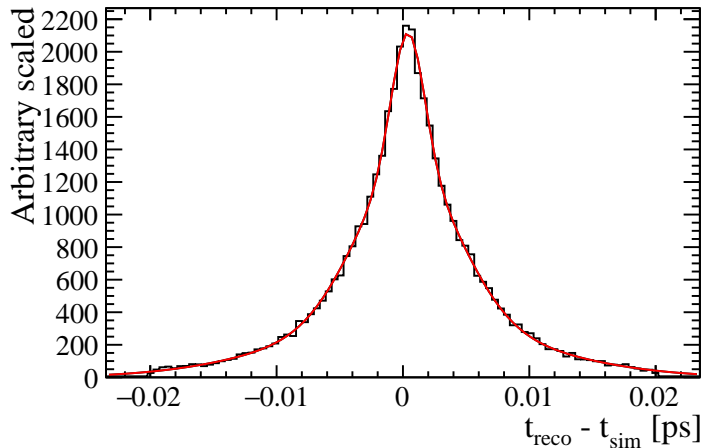


Figure 3: distribution of  $t_{reco} - t_{sim}$ . The distribution is fitted with the sum of three Gaussian functions with equal mean.

### 3 Results and discussion

Table 1: Parameters summary table

	LHCb(HL-LHC)	CEPC(Tera-Z)	CEPC/LHCb
$bb$ statics	$43.2 \times 10^{12}$	$0.152 \times 10^{12}$	1/284
Acceptance $\times$ efficiency	7%	75%	10.7
Br	$6 \times 10^{-6}$	$12 \times 10^{-6}$	2
Flavour tagging*	4.7%	20%	4.3
Time resolution* ( $\exp(-\frac{1}{2}\Delta m_s^2 \sigma_t^2)$ )	0.52	1	1.92
scaling factor $\xi$	0.0014	0.0019	0.8
$\sigma(\phi_s)$	3.3 mrad	4.3 mrad	

Our simulations and estimates show that in future  $Z$ -factories, the proper decay time resolution can reach 4.7 fs, the detector acceptance $\times$ efficiency can

be as good as 75%, and the flavor tagging power can be 20%. Assuming that the future  $Z$ -factory will operate in Tera- $Z$  mode (i.e.,  $10^{12}$   $Z$  will be produced), the scaling factor  $\xi_{FE}$  is 0.0019. The expected  $\phi_s$  resolution is  $\sigma(\phi_s, FE) = \xi_{FE} \times \sigma(\phi_s, \text{LHCb})/\xi_{\text{LHCb}} = 4.3$  mrad, which is competitive to 3.3 mrad, the expected  $\phi_s$  measurement resolution of LHCb at the High-Luminosity LHC.

Figure 4 shows the resolution ratio of  $\phi_s$  as a function of the tagging power and decay time resolution. The baseline resolution is with the parameters described above. The dashed red line represents the ratio for  $\Gamma$  or  $\Delta\Gamma$  resolution, and the solid black line represents the ratio for  $\phi_s$  resolution. The ratio of  $\phi_s$  is calculated analytically and the resolution of  $\Delta\Gamma$  is from the toy Monte Carlo study. The ratio of  $\Gamma$  is expected to be the same as that of  $\Delta\Gamma$ .

It is shown that when the tagging power is optimized to 30%, the  $\phi_s$  precision can be improved by another 20%. The current time resolution is already good enough and reaches the saturation point.

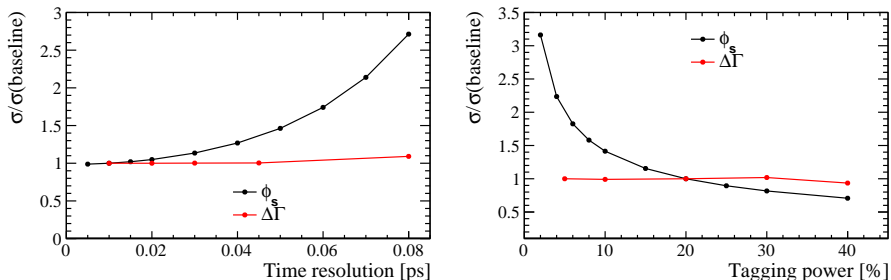


Figure 4: The expected resolution of  $\phi_s$  varies with the resolution of the proper decay time (left) and tagging power (right). The resolution is shown as the ratio between the baseline calculation and the varied calculation.

The weak dependence of tagging power and decay time on  $\Gamma$  and  $\Delta\Gamma$  means that the 4.3 times better flavor tagging power and 1.92 times better time resolution factor of CEPC, in contrast to  $\phi_s$ , have no effect on these observables. The estimated resolution is  $0.24 \text{ ns}^{-1}$  for  $\Delta\Gamma$  and  $0.072 \text{ ns}^{-1}$  for  $\Gamma$ . Note that the measured resolution of  $\Gamma_s - \Gamma_d = 0.0024 \text{ ps}^{-1}$ [10] is taken as the resolution of  $\Gamma$  for the projection.

Figure 3 shows the expected confidential range (68% confidential level) of  $\Delta\Gamma - \phi_s$ . The black dot in the paper is the prediction of the standard model. The red and blue circles represent the expected precision of Tera- $Z$  CEPC and LHCb at the High-Luminosity LHC. The expected precision of  $\phi_s$  at the future  $Z$ -factory is competitive with future hadron colliders. These results change our mind about the measurement of flavor physics at the  $Z$  pole. It is usually believed that the advantage of the electron position machine over the hadron collider is the decay channel with the neutrino, since the neutrino can be reconstructed at the electron position collider with missing energy. However, as shown in Table 1, the statistical disadvantage of the Tera- $Z$   $Z$  factory can be

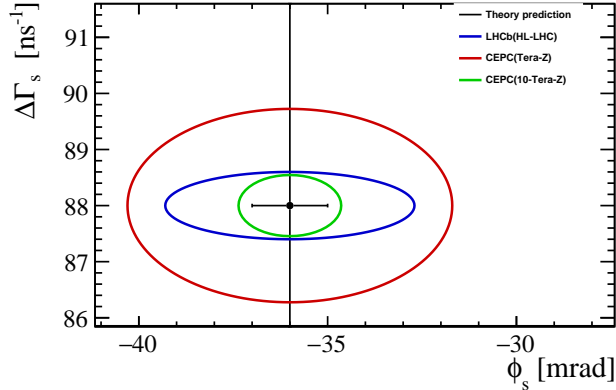


Figure 5: expected confidential region (68% confidential level) of  $\Delta\Gamma - \phi_s$ . The black dots in the paper is the Standard Model prediction. The red and blue circle represents the expected precision of Tera- $Z$  CEPC and LHCb on High-Luminosity LHC. The green circle represents the expected precision of 10-Tera- $Z$  CEPC. The black point represents the current standard model prediction. All the circles are centered at the standard model central value.

overcome with a much cleaner environment, good PID, and accurate track and vertex measurement. Without the benefits of flavor tagging and time resolution, the  $\Gamma$  and  $\Delta\Gamma$  resolution is much worse than expected for the LHC at high-luminosity. Only with the 10-Tera- $Z$   $Z$  factory can the expected resolution of  $\Delta\Gamma$  and  $\Gamma$  be competitive. This represents a requirement for the future  $Z$ -factory.

Particle identification is found to be critical in this study. It is found that tagging performance degrades rapidly when particles are incorrectly identified. And with the particle identification information, the different hadrons can be distinguished to achieve a cleaner environment. The resolution of the vertex reconstruction determines the proper resolution of the decay time. It is found that the resolution is good enough to reach the saturation point. However, a good vertex reconstruction is required to rule out combinatorial backgrounds.

## Acknowledgements

We would like to thank Jibo He, Wenbin Qian, Yuehong Xie, and Liming Zhang for the help in discussion, polishing the manuscript, and crossing the results.

## References

- [1] N. Cabibbo, “Unitary Symmetry and Leptonic Decays,” *Phys. Rev. Lett.*, vol. 10, pp. 531–533, 1963.
- [2] M. Kobayashi and T. Maskawa, “CP Violation in the Renormalizable Theory of Weak Interaction,” *Prog. Theor. Phys.*, vol. 49, pp. 652–657, 1973.
- [3] M. Neubert, “B decays and the heavy quark expansion,” *Adv. Ser. Direct. High Energy Phys.*, vol. 15, pp. 239–293, 1998.
- [4] G. Aad *et al.*, “Measurement of the  $CP$ -violating phase  $\phi_s$  in  $B_s^0 \rightarrow J/\psi\phi$  decays in ATLAS at 13 TeV,” *Eur. Phys. J. C*, vol. 81, no. 4, p. 342, 2021.
- [5] G. Aad *et al.*, “Flavor tagged time-dependent angular analysis of the  $B_s \rightarrow J/\psi\phi$  decay and extraction of  $\Delta\Gamma_s$  and the weak phase  $\phi_s$  in ATLAS,” *Phys. Rev. D*, vol. 90, no. 5, p. 052007, 2014.
- [6] T. Aaltonen *et al.*, “Measurement of the Bottom-Strange Meson Mixing Phase in the Full CDF Data Set,” *Phys. Rev. Lett.*, vol. 109, p. 171802, 2012.
- [7] V. Khachatryan *et al.*, “Measurement of the  $CP$ -violating weak phase  $\phi_s$  and the decay width difference  $\Delta\Gamma_s$  using the  $B_s^0 \rightarrow J/\psi\phi(1020)$  decay channel in pp collisions at  $\sqrt{s} = 8$  TeV,” *Phys. Lett. B*, vol. 757, pp. 97–120, 2016.
- [8] V. M. Abazov *et al.*, “Measurement of the  $CP$ -violating phase  $\phi_s^{J/\psi\phi}$  using the flavor-tagged decay  $B_s^0 \rightarrow J/\psi\phi$  in  $8 \text{ fb}^{-1}$  of  $p\bar{p}$  collisions,” *Phys. Rev. D*, vol. 85, p. 032006, 2012.
- [9] R. Aaij *et al.*, “Resonances and  $CP$  violation in  $B_s^0$  and  $\bar{B}_s^0 \rightarrow J/\psi K^+ K^-$  decays in the mass region above the  $\phi(1020)$ ,” *JHEP*, vol. 08, p. 037, 2017.
- [10] R. Aaij *et al.*, “Updated measurement of time-dependent  $\Delta\Gamma_s$  CP-violating observables in  $B_s^0 \rightarrow J/\psi K^+ K^-$  decays,” *Eur. Phys. J. C*, vol. 79, no. 8, p. 706, 2019. [Erratum: *Eur.Phys.J.C* 80, 601 (2020)].
- [11] R. Aaij *et al.*, “Measurement of the  $CP$ -violating phase  $\phi_s$  in  $\bar{B}_s^0 \rightarrow D_s^+ D_s^-$  decays,” *Phys. Rev. Lett.*, vol. 113, no. 21, p. 211801, 2014.
- [12] R. Aaij *et al.*, “First study of the  $CP$  -violating phase and decay-width difference in  $B_s^0 \rightarrow \psi(2S)\phi$  decays,” *Phys. Lett. B*, vol. 762, pp. 253–262, 2016.
- [13] R. Aaij *et al.*, “Measurement of the  $CP$ -violating phase  $\phi_s$  from  $B_s^0 \rightarrow J/\psi\pi^+\pi^-$  decays in 13 TeV  $pp$  collisions,” *Phys. Lett. B*, vol. 797, p. 134789, 2019.
- [14] C. S. Group *et al.*, “Cepc conceptual design report: Volume 2-physics & detector,” *arXiv preprint arXiv:1811.10545*, 2018.

- [15] W. K. et al., “Simulating Multi-Particle Processes at LHC and ILC,” 2011.
- [16] T. Sjöstrand, “Pythia,” 2005.
- [17] S. Agostinelli, J. Allison, K. a. Amako, J. Apostolakis, H. Araujo, P. Arce, M. Asai, D. Axen, S. Banerjee, G. . Barrand, *et al.*, “Geant4-a simulation toolkit,” *Nuclear instruments and methods in physics research section A: Accelerators, Spectrometers, Detectors and Associated Equipment*, vol. 506, no. 3, pp. 250–303, 2003.